ELSEVIER

Biophysical Chemistry 122 (2006) 50–57

Biophysical Chemistry

http://www.elsevier.com/locate/biophyschem

Voltage-dependent energetics of alamethicin monomers in the membrane

Madhusoodanan Mottamal, Themis Lazaridis *

Department of Chemistry, City College of New York/CUNY, 138th St. and Convent Ave, New York, NY 10031, USA

Received 10 January 2006; received in revised form 11 February 2006; accepted 11 February 2006
Available online 15 March 2006

Abstract

The implicit membrane model IMM1 is extended to include the effect of transmembrane potential and used to investigate the optimal membrane binding configurations and energies for alamethicin helices. In the absence of voltage, the lowest energy configuration is on the membrane surface with a tilt allowing the N terminus to be fully buried. Slightly higher in energy is an also tilted configuration with the N terminus deeper in the membrane and almost crossing the membrane. In 26 Å membranes and in the presence of 0.1 V voltage, the TM orientation becomes lower in energy. This is consistent with the assumption that voltage induces a transition from the interfacial to the inserted (TM) orientation. This effect of voltage is smaller in thicker membranes. The results are compared to previous experimental and theoretical studies and the findings are discussed in relation to the mechanism of channel formation by alamethicin.

Keywords: Transmembrane potential; Alamethicin; Voltage-dependent gating; Implicit membrane model

1. Introduction

Peptaibols are fungal peptides rich in α-aminoisobutyric acid (Aib) and include over 300 currently known sequences (see http://www.cryst.bbk.ac.uk/ peptaibol). The best studied of these is alamethicin (ALM), which forms weakly cation-specific ion channels in membranes and has served as a simple model for ion channels [1,2]. The structure of ALM in crystals is a bent α-helix [3]. Conductivity is voltage dependent and appears in bursts of different magnitude, which suggests that transient pores may be forming consisting of a variable number of monomers. Ion conductivity is largest when ALM is added to the +side of the membrane.

The most widely accepted mechanism for alamethicin action is the "barrel-stave" model, in which several ALM helices in an orientation parallel to the membrane normal cluster together forming a cylinder filled with water through which ions can flow. Biophysical studies with model membranes find either an interfacial [4] or a transmembrane [5] orientation depending on conditions [6]. Various propositions have been made for the voltage dependent step: partition into the bilayer, transition from an interfacial to a transmembrane orientation, conformational change, further immersion into the bilayer, flipping of helices from an antiparallel to a parallel orientation, or aggregation [2,7,8].

Quite a few molecular simulation studies have been reported, primarily by the Sansom group [9–18] but they have not reported relative free energies of different conformations. Continuum solvent studies predicted the transmembrane orientation to be slightly more favorable than the interfacial one [19]. Lately, research activity on ALM has somewhat abated, perhaps because existing techniques have reached their limits.

Despite the numerous studies on alamethicin and other peptaibols, a number of important questions still remain, for example: a) What is the voltage dependent step in ALM pore formation? b) Does the barrel-stave mechanism apply to the 16-residue peptaibols, which seem to be too short to span the bilayer? Some of them exhibit multiple level conductance states, like alamethicin, and some do not [1]. c) What is the role of the conserved Pro and the resulting kink in the middle of peptaibols? Analogs with the Pro replaced by Ala exhibited similar voltage gating but a smaller number of monomers per channel and shorter open channel lifetimes [8]. This work addresses the first of the above questions. We extend the IMM1 implicit membrane model to incorporate transmembrane potential using an analytical solution of the Poisson Boltzmann

* Corresponding author. Tel.: +1 212 6508364; fax: +1 212 650 6107.
E-mail address: tlazaridis@ccny.cuny.edu (T. Lazaridis).

0301-4622/$ - see front matter © 2006 Elsevier B.V. All rights reserved.
doi:10.1016/j.bpc.2006.02.005

equation for planar membrane potential and apply it to the monomeric state of Alamethicin.

2. Methods

Over the past 3 years we have developed an effective energy function for proteins in lipid membranes [20] based on the EEF1 energy function for water-soluble proteins [21,22]. Effective energy (or potential of mean force, W) is the free energy of a given, fixed protein conformation and is equal to the intramolecular energy, obtained from a standard force field, plus the solvation free energy:

$$W = E + \Delta G^{\mathrm{slv}} \tag{1}$$

E is obtained from the extended atom (param19) CHARMM force field [23,24], where all atoms are represented explicitly except for the hydrogens that are bonded to nonpolar carbons. The theoretical foundation of the concept of effective energy and the distinction between effective energy and free energy are discussed in Ref. [25].

EEF1 aims to describe the effective energy of proteins in water. It differs from the standard CHARMM force field in two ways: a) an implicit solvation term is added that describes the interaction of each atom with the solvent, and b) the ionic sidechains are neutralized and a distance dependent dielectric constant ($\varepsilon = r$) is used for the electrostatic interactions. The implicit solvation term has the form:

$$\Delta G^{\mathrm{slv}} = \sum_i \Delta G_i^{\mathrm{slv}} = \sum_i \Delta G_i^{\mathrm{ref}} - \sum_i \sum_{j \neq i} f_i(r_{ij}) V_j \tag{2}$$

where $\Delta G_i^{\mathrm{slv}}$ is the solvation free energy of atom i and r_{ij} is the distance between i and j. Eq. (2) says that the solvation free energy of atom i is equal to that in a small model system where the atom is fully exposed to solvent ($\Delta G_i^{\mathrm{ref}}$) minus the solvation free energy it loses due to the presence of surrounding atoms. The solvation free energy density f is modeled as a Gaussian function

$$f_i(r) 4\pi r^2 = \alpha_i \exp(-x_i^2), \qquad x_i = \frac{r - R_i}{\lambda_i} \tag{3}$$

where R_i is the van der Waals radius of i, λ_i is a correlation length (3.5 Å for most atoms), and α_i is given by

$$\alpha_i = 2\Delta G_i^{\mathrm{free}} / \sqrt{\pi} \lambda_i \tag{4}$$

where $\Delta G_i^{\mathrm{free}}$ is the solvation free energy of the free (isolated) atom i; $\Delta G_i^{\mathrm{free}}$ is close but not identical to $\Delta G_i^{\mathrm{ref}}$ and is determined by requiring that the solvation free energy of deeply buried atoms be zero.

Calculations of the potential of mean force between ionizable sidechains in water [26] showed that EEF1 overestimates the attraction between unlike charged and hydrogen bonding groups. In addition, as was originally reported [21], certain interactions involving arginine were not correct. Thus we proposed a modified set of partial charges for the ionizable and polar sidechains designed to optimize the agreement with the calculated potentials of mean force. This updated version of the energy function is referred to as EEF1.1.

IMM1 (Implicit Membrane Model 1) is an extension of EEF1 to heterogeneous membrane–water systems. For molecules immersed in a membrane the values $\Delta G_i^{\mathrm{ref}}$ must correspond to a nonaqueous phase. Since data for the solvation free energy of molecules in the hydrocarbon core of membranes are not available (such data are available for partition at the membrane interface [27]), we used data for the distribution of amino acid sidechain analogues between cyclohexane and the gas phase [28]. The membrane is considered to be parallel to the xy plane with its center at $z = 0$. The solvation parameters of all atoms ($\Delta G_i^{\mathrm{ref}}$ and $\Delta G_i^{\mathrm{free}}$) now depend on the vertical direction, z, or $z' = |z|/(T/2)$, where T is the thickness of the nonpolar core of the membrane:

$$\Delta G_i^{\mathrm{ref}}(z') = f(z') \Delta G_i^{\mathrm{ref,\ wat}} + (1 - f(z')) \Delta G_i^{\mathrm{ref,\ chex}}. \tag{5}$$

The function $f(z')$ describes the transition from one phase to the other:

$$f(z') = \frac{z'^n}{1 + z'^n} \tag{6}$$

where n controls the steepness of the transition. The exponent $n = 10$ gives a region of 6 Å over which the environment goes from 90% nonpolar to 90% polar. This corresponds roughly to X-ray and neutron diffraction data for the structure of the lipid bilayers [29]. The midpoint of the transition ($f = 0.5$) corresponds to the hydrocarbon–polar headgroup interface. Hence, as in most other hydrophobic slab models, the headgroup region is assumed to have the same properties as aqueous solution.

To account for the strengthening of electrostatic interactions in the membrane in a way that is compatible with the distance dependent dielectric used in EEF1 we introduced a modified dielectric screening function

$$\varepsilon = r^{f_{ij}} \tag{7}$$

where f_{ij} depends on the position of the interacting atoms with respect to the membrane. Far from the membrane, f_{ij} is equal to 1 so that we recover the linear distance-dependent dielectric model. The model

$$f_{ij} = \sqrt{f_i f_j} \tag{8}$$

with f_i, f_j given by Eq. (6), which gives $\varepsilon = 1$ in the center of the membrane was found to strengthen electrostatic interactions too much. Therefore, we employed the empirical model

$$f_{ij} = a + (1 - a)\sqrt{f_i f_j} \tag{9}$$

with a an adjustable parameter. It was found that the value $a = 0.85$ gives reasonable results.

IMM1 was recently extended to account for the presence of net charge on the membrane surface (surface potential) [30]. The effect of surface potential was described using the Gouy–Chapman theory, which assumes that the charge is smeared on the membrane, solves analytically the 1-dimensional Poisson–Boltzmann equation, and yields the electrostatic potential as a

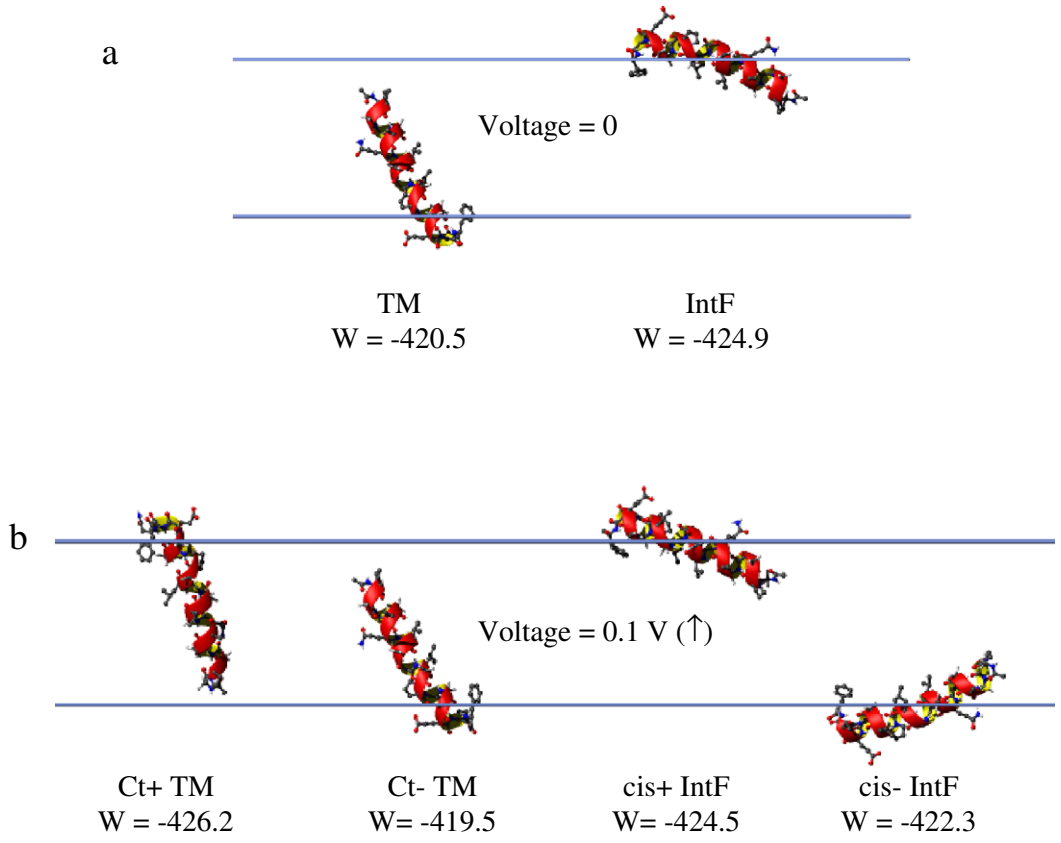

Fig. 1. Structures obtained after 1 ns dynamics and energy minimization starting from perpendicular or parallel to membrane initial orientations. The membrane width is 26 Å. The voltage is positive on the upper side of the membrane. a) No voltage, b) voltage=0.1 V (+upwards).

function of distance from the membrane. Then an extra term is added to our energy function that describes the interaction of the peptide charges with the surface potential:

$$E_{GC} = \sum \phi_i q_i \tag{10}$$

where ϕ_i is the potential and q_i the charge of atom i. The user specifies the mole fraction of anionic lipids, the area per lipid, the salt concentration, the valence of the electrolyte, and the position of the plane of smeared charge relative to the nonpolar/polar interface. From these the surface charge is calculated and used in the Gouy–Chapman equations. Modeling of proteins with an aqueous pore is also possible [31].

Here we extend IMM1 by incorporating the effect of transmembrane potential. For a planar membrane an analytical solution of the Poisson–Boltzmann equation gives [32]

$$z < -T/2 \;\; \phi(z) = A\exp(\kappa(z + T/2))$$

$$-T/2 < z < T/2 \;\; \phi(z) = A\left[\frac{\varepsilon_w}{\varepsilon_m}\kappa(z + T/2) + 1\right]$$

$$z > T/2 \;\; \phi(z) = V - A\exp(-\kappa(z - T/2)) \tag{11}$$

where $A = V\left[2 + \frac{\varepsilon_w}{\varepsilon_m}\kappa T\right]^{-1}$, ε_m is the permittivity of the membrane, T is the thickness, V is the transmembrane potential, and κ is the inverse Debye length. This equation is not exact in the case of a large membrane protein protruding from the membrane, but it should be a reasonable first approximation. The energy is given by a term similar to Eq. (10).

The above functions has been incorporated into the program CHARMM [23]. The presence of voltage breaks the symmetry of IMM1 with respect to the xy plane. Until now the function depended only on $|z|$. In the CHARMM implementation, positive voltage has been assigned to the positive z axis. New CHARMM residues were created for Aib and the terminal Phl (phenylalaninol).

3. Results

We have used IMM1 with transmembrane voltage to obtain data on the energetics of different alamethicin orientations on a membrane and the effect of transmembrane voltage. In the presence of voltage, which is positive in the positive z direction, the two sides of the membrane are no longer equivalent. When ALM is on the $+z$ side, we call this the cis+ interfacial position; the opposite is called cis− interfacial. The transmembrane orientation with the C terminus in the $+z$ direction is called Ct+ transmembrane; the opposite Ct− transmembrane. ALM contains only one negative charge (Glu 18), which is towards

Table 1
Minimized and average (over the last 0.4 ns) effective energies (kcal/mol) of the structures depicted in Fig. 1

Medium/voltage/ALM orientation	Minimized energy	Average energy
Water	−413.1	
Lipid Bilayer		
V=0, TM	−420.5	−280.0±2.0
V=0, IntF	−424.9	−281.2±1.8
V=0.1, cis+ IntF	−424.5 (E_{volt}=−2.6)	−282.6±2.3
V=0.1, cis− IntF	−422.3 (E_{volt}=+0.3)	−280.2±1.8
V=0.1, Ct+ TM	−426.2 (E_{volt}=−3.4)	−284.6±2.1
V=0.1, Ct− TM	−419.5 (E_{volt}=+0.8)	−280.2±2.0

E_{volt} is the contribution of transmembrane potential to the energy (interaction of the peptide with the electric field). Error bars are standard deviations.

the C terminus. In the presence of voltage this negative charge will prefer to be in the +direction.

The structure of alamethicin (mostly α-helical) was obtained from the PDB (1AMT), placed at either transmembrane or interfacial orientations on either side of the membrane and subjected to 1 ns MD simulation. No internal constraints were used in the simulations. The final structures from the simulations were energy-minimized and their energies were compared. Fig. 1a shows the two final structures in the absence of voltage and Fig. 1b the four final structures in the presence of 0.1 V voltage. We see that the peptide adopts two types of orientations: a tilted orientation at the interface with the N terminus partially inserted and an also tilted, more fully inserted, TM orientation, with the N terminus almost crossing the membrane. A buried N terminus is not energetically forbidden for ALM because it is acetylated and contains Pro and Aib, i.e., fewer polar groups are desolvated upon membrane insertion than in usual helices. These results are in agreement with the suggestion that ALM penetrates the hydrophobic core of the bilayer even in the absence of voltage [7]. Voltage does not produce significant changes in these structures but affects the relative energetics.

Table 1 shows the minimized and average effective energies of these structures. The transfer energy from water to the membrane is large enough to ensure that all ALM partitions to the membrane at reasonable concentrations. Therefore, partitioning to the membrane is unlikely to be the voltage-dependent step. Both minimized and average energies show that in the absence of voltage, the tilted interfacial structure is lower in energy than the TM structure. In the presence of voltage, the positions where Glu18 is on the +side (cis+ and Ct+) have lower energies than the other two, as expected, and the TM orientation is energetically more favorable than the interfacial orientation. This is consistent with the proposition that voltage induces a transition from the interfacial to the inserted position.

One difficulty in these results is that the noise in the simulations is comparable to the energy difference between the two orientations. Therefore, to test the reproducibility of the results, we considered three more interfacial orientations by rotating the peptide around its helix axis by 90°, 180° and 270° and performed 1 ns simulations in the presence and absence of voltage. In all cases, the final structures had hydrophobic residues facing the hydrophobic core of the membrane and hydrophilic residues either in the headgroup region or in the aqueous medium. The average and minimized energies of all these interfacial structures in the absence of voltage were lower than those of the TM structures. In the presence of voltage, the energies of all the interfacial structures were higher than those of the Ct+ TM structure. Thus, different initial interfacial orientations give similar results.

The simulations show that the two orientations correspond to local minima. To understand the nature of the barrier between them, the effective energy of ALM is plotted as a function of tilt angle in Fig. 2. Starting from the Ct+ TM structure (Fig. 1), the tilt angle is changed at 5° intervals from 0° to 90° keeping the peptide rigid. The orientations of ALM

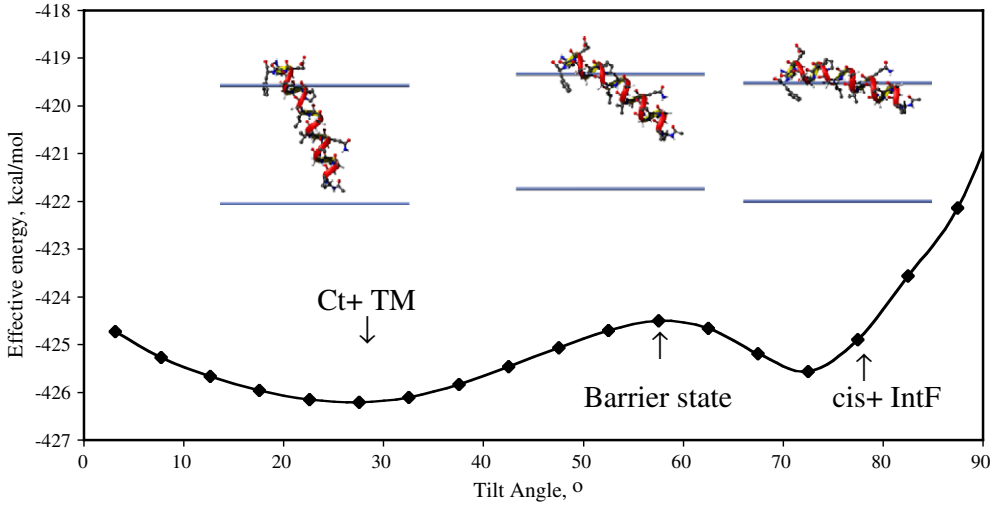

Fig. 2. Effective energy of ALM in a lipid bilayer (thickness=26 Å) at different tilt angles in the presence of voltage (0.1 V). Arrows indicate the orientations of ALM that correspond to the Ct+TM and cis+IntF orientations in Fig. 1.

Table 2
Effective energy (kcal/mol) of ALM in different states along the reaction path (Fig. 2)

Orientation of ALM and its tilt angle	Effective energy (vdw, elec, solv)
Ct+ TM (27°)	−426.2 (−71.2, −316.7, −83.8)
Barrier state (~58°)	−424.5 (−71.2, −313.7, −85.0)
Cis+ IntF (~78°)	−424.9 (−71.2, −304.6, −94.6)

For this calculation the peptide is kept rigid. E_{volt} is included in the solvation free energy.

that correspond to the Ct+ TM and to the cis+ IntF structure in Fig. 1 are marked with arrows. The Ct+ TM orientation has a tilt angle of ~27°. The energy barrier along the transition path is about 1.7 kcal/mol occurs around 58°. Table 2 shows the effective energy of ALM at the Ct+ TM, barrier, and cis+ IntF states along the reaction path. The cis+ IntF orientation has lower solvation free energy (ΔW_{solv} = −10.8 kcal/mol) and higher electrostatic energy (ΔW_{elec} = +12.1 kcal/mol) than the Ct+ TM. The barrier is due to incomplete compensation between the electrostatic and solvation terms. The electrostatic energy of the barrier state is ~3.0 kcal/mol higher than the Ct+ TM orientation due to the differences in the electrostatic interaction energies of residues 10–16 when they move towards the membrane surface from the hydrophobic core of the membrane, whereas the solvation energy is more favorable for the barrier state by −1.2 kcal/mol. This favorable solvation energy is due to Gly11 and Gln7 approaching the membrane surface.

To examine the effect of membrane thickness on the optimal orientation of ALM in the absence and presence of voltage, simulations were also done with a hydrophobic membrane thickness of 30 Å. The resulting peptide orientations (figure not shown) were the same as in Fig. 1. Table 3 shows the minimized and average energies of the peptide. In the absence of voltage, the minimized energy of the tilted interfacial structure is ~3.0 kcal/mol lower than the TM orientation. The average energy is also more favorable (~1 kcal/mol) for the interfacial orientation. In the presence of voltage, the minimized energies still favor the IntF cis+ orientation, while the average energies for the IntF cis+ orientation and the TM Ct+ orientation are the same (−281.9 kcal/mol). Thus the transition from the IntF cis+ orientation to TM Ct+ orientation is somewhat more difficult in thicker membranes.

Table 3
Minimized and average (over the last 0.4 ns) effective energies (kcal/mol) of the structures of ALM in a membrane thickness of 30 Å

Medium/voltage/ALM orientation	Minimized energy	Average energy
Water	−413.1	
Lipid Bilayer		
V=0, TM	−422.9	−279.1±2.1
V=0, IntF	−425.9	−280.2±2.2
V=0.1, cis+ IntF	−425.3 (E_{volt}=−3.1)	−281.9±2.3
V=0.1, cis− IntF	−423.5 (E_{volt}=+0.9)	−279.6±2.4
V=0.1, Ct+ TM	−423.9 (E_{volt}=−2.6)	−281.9±1.8
V=0.1, Ct− TM	−422.4 (E_{volt}=+0.3)	−278.1±2.0

Table 4
Effective energy of the Ct+ TM and cis+ IntF (Fig. 1) structures with a regular glutamic acid (Glu) and a modified glutamic acid (Glu^0) with neutralized –COO- group

	With Glu		With Glu^0	
	Voltage 0.1 V	No Voltage	Voltage 0.1 V	No Voltage
Ct+ TM	−426.2	−422.8	−422.2	−421.0
cis+ IntF	−424.5	−421.9	−420.6	−420.3
ΔW (TM− IntF)	−1.7	−0.9	−1.6	−0.7
$\Delta\Delta W$	−0.8		−0.9	

To examine the role of the single Glu residue in the shift towards the TM orientation in the presence of voltage, the energetics of the final Ct+ TM and cis+ IntF structures in Fig. 1 were also calculated in the presence and absence of voltage with a modified $Glu^0$18 with a neutralized carboxylic sidechain (see Table 4). For this modified peptide, voltage affects the relative energetics of the two conformations only through its interaction with the helix dipole. The shift towards the TM configuration is similar for the wild type and modified peptide (0.8–0.9 kcal/mol), which means that the Glu does not play a role in the shift towards the TM configuration induced by V. The shift of 0.8–0.9 kcal/mol contributed by the helix dipole is close to the theoretical value obtained by multiplying the dipole moment (~70D) by the electric field (0.1 V/26 Å), which is −1.3 kcal/mol. This value is probably a better estimate of the shift, because MD values inevitably have statistical uncertainties.

4. Discussion

In this work the effect of transmembrane potential was incorporated into the IMM1 implicit membrane model by using an analytical solution of the Poisson–Boltzmann equation. Although this model cannot capture the full complexity of a lipid membrane, it offers three important advantages: computational speed, rapid equilibration, and the ability to compare the energetics of different configurations. The model was applied to alamethicin monomers. The major findings are a) ALM binds strongly to the membrane ($\Delta W_{water \rightarrow membrane}$ is ~−12 kcal/mol; consistent with the observation that ALM binds strongly lipid bilayers [33].) b) in the absence of voltage the optimal orientation of ALM is interfacial c) in the presence of voltage the optimal orientation is transbilayer d) increase in thickness weakens the effect of voltage on the optimal orientation.

These findings are in contrast to the results of a Poisson–Boltzmann implicit membrane calculation, which found the transmembrane orientation to be optimal in the absence of voltage [19]. The two approaches treat both the hydrophobic effect and electrostatics very differently and can easily produce different results for orientations that are so close in energy. In addition, the ability to do MD simulations with IMM1 may have allowed some local adjustments (such as partial insertion of the N terminus) that tipped the balance towards the interfacial structure. An earlier, simpler implicit membrane model also

found the TM orientation to be favored even in the absence of voltage [34]. In that model the lifetime of the interfacial orientation was found to be about 0.12 ns in the absence of voltage and it decreased when the bilayer potential was applied [34]. In contrast, in our model the initial interfacial orientation of the peptide remained interfacial throughout the 1 ns simulation. A longer simulation (2 ns) also showed the same result.

A large variety of experimental data exist on ALM–membrane interactions. An NMR study showed that ALM interacts primarily at the water–lipid interface without significant insertion into the bilayer in the absence of voltage [4]. However, CD data in unilamellar vesicles suggested that ALM incorporates into the lipid [35]. Oriented CD in multilamellar samples showed an interfacial orientation at low peptide/lipid ratio and an inserted state at higher ratios [6,36]. Site directed spin-labeling studies show that ALM is in a linear form (not bent closed form) as in the crystal structure [3] and inserts along the bilayer normal with its C-terminus in the aqueous region and N the terminus in the membrane hydrocarbon region even in the absence of voltage [37]. This is similar to our TM structure, although in our studies this structure is favored only in the presence of voltage. The energy difference between the interfacial and TM structures is apparently very small. Thus, slight differences in experimental setup might tip the balance towards one or the other. 15N NMR studies showed a tilted orientation of ALM in the bilayer in the nonconductive state [38]. The tilt was between 10° and 20°. This is similar to our TM structure, whose tilt is 27°. It should also be noted that the orientation of ALM is sensitive to the physical state of the bilayer [1].

Several experimental studies explored the effect of membrane thickness on ALM insertion. ALM was found to insert better in DPPC than in ether-linked DHPC bilayers, presumably because of the matching of the hydrophobic thickness of the DPPC bilayer (24 vs. 13 Å of DHPC) with the hydrophobic length of ALM [39]. Circular dichroism measurements also showed less favorable interaction of the peptide with thicker membranes [33]. NMR studies showed that as the hydrophobic thickness of the membrane increased, ALM oriented predominantly parallel to the surface [40]. This is consistent with our finding that increase of hydrophobic thickness from 26 to 30 Å shifts the equilibrium towards the surface state. Our study also shows that in a thinner membrane the effect of voltage is more prominent than in a thicker membrane. A mechanism for peptide-induced pore formation due to membrane thinning has been suggested using spectroscopic studies

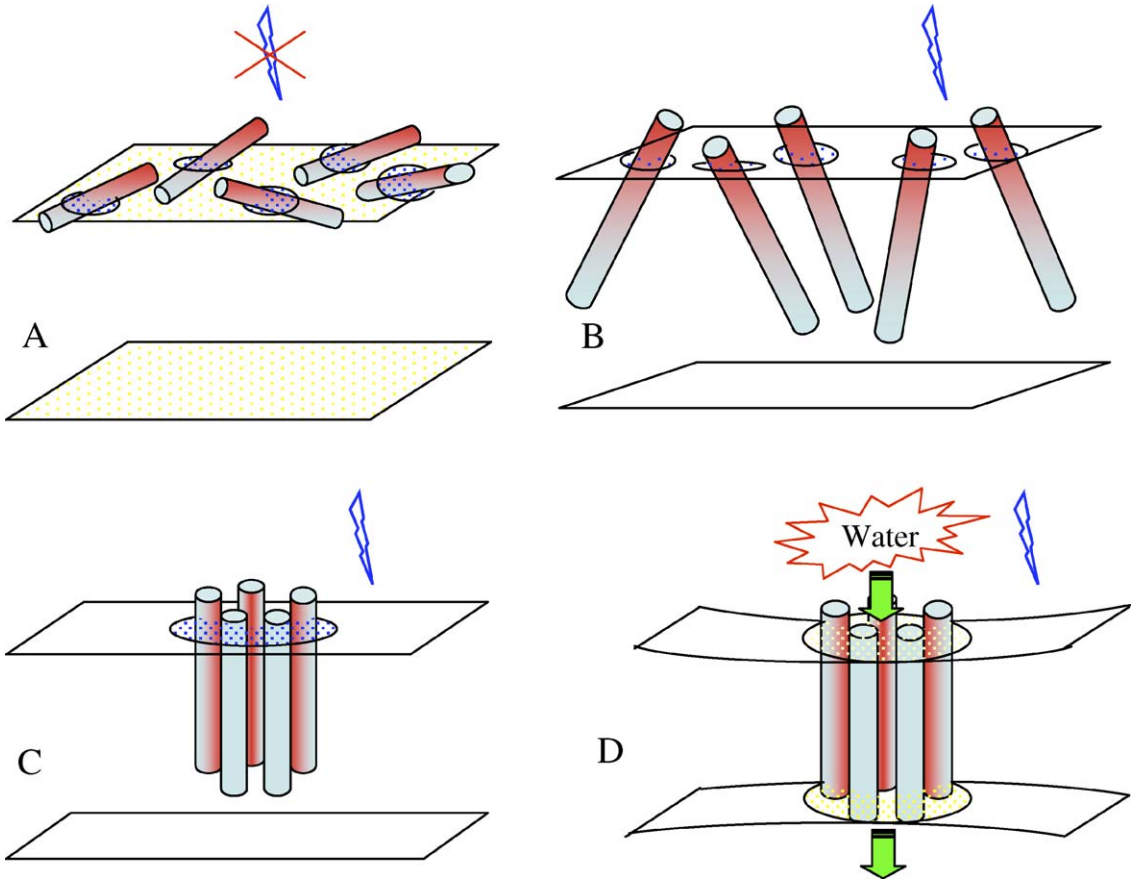

Fig. 3. A four stage model for the pore formation of alamethicin with 5 helix bundle in the presence of a transmembrane potential. Red color in stages 1 (A) and 2 (B) represents the hydrophilic C-terminus, and in stages 3 (C) and 4 (D) represent the hydrophilic surface. Voltage is represented with lightning bolt and deformed membrane surface is represented with curved surface. (For interpretation of the references to colour in this figure legend, the reader is referred to the web version of this article.)

[41]. Localized thinning of the membrane promoted by the peptide was also observed in an EPR study [37,42]. In our simulations, deformation of the bilayer surrounding the peptide is not modeled, although it would be possible to account for it indirectly [19,43].

It is experimentally known that channel formation is much more facile when ALM is added to the positive side of the transmembrane voltage [44]. The explanation of this is straightforward: for a favorable interaction with the applied voltage, the negatively charged Glu18 has to be on the +V side (the effective energy of Ct+ TM structure is lower than the CT− TM orientation). Then, channel formation from the trans side would require the hydrophilic C terminus to cross the membrane, and that is energetically unfavorable. In contrast, the hydrophobic N terminus crosses the membrane easily. This is consistent with experiments on Alm analogs where the negative charge at the C terminus was eliminated or a charge was inserted at the N terminus [1].

A number of mechanisms have been suggested for the voltage-dependent step in alamethicin channels gating [2]: 1) conformational change, 2) flipping of helices, 3) partitioning from solution into the membrane, 4) transition from a surface-bound to an inserted orientation. Our study did not show any conformational change of the peptide in the presence of voltage. Voltage dependent flipping of the peptide would require desolvation of the hydrophilic C-terminus as it crosses the membrane, and this process has a high energy barrier. In the voltage-dependent partitioning model, partitioning of the peptide between the membrane and aqueous phase requires diffusion of the peptide into the membrane. However, our calculations, and experiments [5,33,35,37,38], show that ALM strongly partitions into the membrane regardless of voltage.

Our results are consistent with the voltage dependent insertion model. An elaboration of this mechanism based on the present results is shown in Fig. 3 for a five-helix bundle, although the number of helices can vary from 4 to 11 [7]. In Stage 1, monomeric ALM adopts a partially N-terminal inserted interfacial orientation in the absence of voltage (Fig. 3.A). Hydrophilic c-termini (red) are oriented outside the hydrophobic core of the membrane. Interaction of ALM with the membrane surface helps to stabilize its helical conformation relative to the peptide in aqueous solution. In stage 2, voltage alters the orientation of ALM to a slightly tilted transmembrane orientation with its hydrophilic Cterminus at the +V side (Fig. 3.B). In this stage, the peptides do not cross the membrane and the deformation of the lipid bilayers is minimal. Stage 3 involves association of the lipid-solvated alpha helical peptide (Fig. 3.C). Lateral association of the peptides is enhanced by the interhelical interaction between Gln7, Glu18, Gln19 (hydrophilic convex surface). The importance of Gln7 inter-helix hydrogen bonds is evident from mutational studies where Q7A substitution was found to abolish channel formation [45]. Here again the peptides do not cross the bilayer completely. In stage 4, the “dry” helix bundle transiently opens up and the inner phase of the bundle gets solvated by water (Fig. 3.D). This process produces thinning of the membrane around the helical bundle to allow the pore water to interact with the other side. Thinning of membranes has been reported in many studies[16,19,46,47].

Future work will involve studies of oligomerization and pore formation by ALM helices.

Acknowledgments

This work was supported by the National Science Foundation (MCB-0316667).

References

[1] M.S. Sansom, The biophysics of peptide models of ion channels, Prog. Biophys. Mol. Biol. 55 (1991) 139–235.
[2] D.S. Cafiso, Alamethicin: a peptide model for voltage gating and protein membrane interactions, Annu. Rev. Biophys. Biomol. Struct. 23 (1994) 141–165.
[3] R.O. Fox Jr., F.M. Richards, A voltage-gated ion channel model inferred from the crystal structure of alamethicin at 1.5 A resolution, Nature 300 (1982) 325–330.
[4] U. Banerjee, R. Zidovetzki, R.R. Birge, S.I. Chan, Interaction of alamethicin with lecithin bilayers: a 31P and 2H NMR study, Biochemistry 24 (1985) 7621–7627.
[5] C.L. North, M. Barranger-Mathys, D.S. Cafiso, Membrane orientation of the N-terminal segment of alamethicin determined by solid-state 15N NMR, Biophys. J. 69 (1995) 2392–2397.
[6] H.W. Huang, Y. Wu, Lipid–alamethicin interactions influence alamethicin orientation, Biophys. J. 60 (1991) 1079–1087.
[7] M.S. Sansom, I.D. Kerr, I.R. Mellor, Ion channels formed by amphipathic helical peptides, a molecular modeling study, Eur. Biophys. J. 20 (1991) 229–240.
[8] H. Duclohier, H. Wroblewski, Voltage-dependent pore formation and antimicrobial activity by alamethicin and analogues, J. Membr. Biol. 184 (2001) 1–12.
[9] M.S. Sansom, D.P. Tieleman, H.J. Berendsen, The mechanism of channel formation by alamethicin as viewed by molecular dynamics simulations, Novartis Found. Symp. 225 (1999) 128–141 (discussion 141–145).
[10] M.S. Sansom, D.P. Tieleman, L.R. Forrest, H.J. Berendsen, Molecular dynamics simulation of membranes with embedded proteins and peptides: porin, alamethicin and influenza virus M2, Biochem. Soc. Trans. 26 (1998) 438–443.
[11] D.P. Tieleman, H.J. Berendsen, M.S. Sansom, Surface binding of alamethicin stabilizes its helical structure: molecular dynamics simulations, Biophys. J. 76 (1999) 3186–3191.
[12] D.P. Tieleman, H.J. Berendsen, M.S. Sansom, An alamethicin channel in a lipid bilayer: molecular dynamics simulations, Biophys. J. 76 (1999) 1757–1769.
[13] D.P. Tieleman, H.J. Berendsen, M.S. Sansom, Voltage-dependent insertion of alamethicin at phospholipid/water and octane/water interfaces, Biophys. J. 80 (2001) 331–346.
[14] D.P. Tieleman, V. Borisenko, M.S.P. Sansom, G.A. Woolley, Understanding pH dependent selectivity of alamethicin K18 channels by computer simulation, Biophys. J. 84 (2003) 1464–1469.
[15] D.P. Tieleman, J. Breed, H.J. Berendsen, M.S. Sansom, Alamethicin channels in membrane: molecular dynamics simulations, Faraday Discuss. 111 (1998) 209–223 (discussion 225–246).
[16] D.P. Tieleman, L.R. Forrest, M.S. Sansom, H.J. Berendsen, Lipid properties and the orientation of aromatic residues in OmpF, influenza M2, and alamethicin systems: molecular dynamics simulations, Biochemistry 37 (1998) 17554–17561.
[17] D.P. Tieleman, B. Hess, M.S. Sansom, Analysis and evaluation of channel models: simulations of alamethicin, Biophys. J. 83 (2002) 2393–2407.

[18] D.P. Tieleman, M.S. Sansom, H.J. Berendsen, Alamethicin helices in a bilayer and in solution: molecular dynamics simulations, Biophys. J. 76 (1999) 40–49.
[19] A. Kessel, D.S. Cafiso, N. Ben-Tal, Continuum solvent model calculations of alamethicin–membrane interactions: thermodynamic aspects, Biophys. J. 78 (2000) 571–583.
[20] T. Lazaridis, Effective energy function for proteins in lipid membranes, Proteins 52 (2003) 176–192.
[21] T. Lazaridis, M. Karplus, Effective energy function for proteins in solution, Proteins 35 (1999) 133–152.
[22] T. Lazaridis, M. Karplus, "New view" of protein folding reconciled with the old through multiple unfolding simulations, Science 278 (1997) 1928–1931.
[23] B.R. Brooks, R.E. Bruccoleri, B.D. Olafson, D.J. States, S. Swaminathan, M. Karplus, CHARMM: a program for macromolecular energy minimization and dynamics calculations, J. Comput. Chem. 4 (1983) 187–217.
[24] E. Neria, S. Fischer, M. Karplus, Simulation of activation free energies in molecular systems, J. Chem. Phys. 105 (1996) 1902–1921.
[25] T. Lazaridis, M. Karplus, Thermodynamics of protein folding: a microscopic view, Biophys. Chem. 100 (2003) 367–395.
[26] A. Masunov, T. Lazaridis, Potentials of mean force between ionizable amino acid sidechains in aqueous solution, J. Am. Chem. Soc. 125 (2003) 1722–1730.
[27] W.C. Wimley, S.H. White, Experimentally determined hydrophobicity scale for proteins at membrane interfaces, Nat. Struct. Biol. 3 (1996) 842–848.
[28] A. Radzicka, R. Wolfenden, Comparing the polarities of the amino acids: sidechain distribution coefficients between the vapor phase, cyclohexane, 1-octanol and neutral aqueous solution, Biochemistry 27 (1988) 1664–1670.
[29] M.C. Weiner, S.H. White, Structure of a fluid dioleoylphosphatidylcholine bilayer determined by joint refinement of X-ray and neutron diffraction data II. Distribution and packing of terminal methyl groups, Biophys. J. 61 (1992) 428–433.
[30] T. Lazaridis, Implicit solvent simulations of peptide interactions with anionic lipid membranes, Proteins 58 (2005) 518–527.
[31] T. Lazaridis, Structural determinants of transmembrane beta-barrels, J. Chem. Theory Comput. 1 (2005) 716–722.
[32] B. Roux, Influence of membrane potential on the free energy of an intrinsic protein, Biophys. J. 73 (1997) 2980–2989.
[33] S. Stankowski, G. Schwarz, Lipid dependence of peptide–membrane interactions, FEBS Lett. 250 (1989) 556–560.
[34] P.C. Biggin, J. Breed, H.S. Son, M.S. Sansom, Simulation studies of alamethicin bilayer interactions, Biophys. J. 72 (1997) 627–636.
[35] G. Schwarz, S. Stankowski, V. Rizzo, Thermodynamic analysis of incorporation and aggregation in a membrane: application to the pore-forming peptide alamethicin, Biochim. Biophys. Acta 861 (1986) 141–151.
[36] F. Chen, M. Lee, H.W. Huang, Sigmoidal concentration dependence of antimicrobial peptide activities: a case study on alamethicin, Biophys. J. 82 (2002) 908–914.
[37] M. Barranger-Mathys, D.S. Cafiso, Membrane structure of voltage-gated channel forming peptides by site-directed spin-labeling, Biochemistry 35 (1996) 498–505.
[38] M. Bak, R.P. Bywater, M. Hohwy, J.K. Thomsen, K. Adelhorst, H.J. Jakobsen, O.W. Sorensen, N.C. Nielsen, Conformation of alamethicin in oriented phospholipid bilayers by 15N solid-state nuclear magnetic resonance, Biophys. J. 81 (2001) 1684–1698.
[39] P.C. Dave, E. Billington, Y.-L. Pan, S.K. Straus, Interaction of alamethicin with ether-linked phospholipid bilayers: oriented circular dichroism, 31P solid-state NMR, and differential scanning calorimetry studies, Biophys. J. 89 (2005) 2434–2442.
[40] B. Bechinger, D.A. Skladnev, A. Orgel, X. Li, E.V. Rogozhkina, T.V. Ovchinnikova, J.D.J. O'Neil, J. Raap, 15N and 31P solid-state NMR investigations on the orientation of zervamicin II and alamethicin in phosphatidylcholine membranes, Biochemistry 40 (2001) 9428–9437.
[41] F.-Y. Chen, M.-T. Lee, H.W. Huang, Evidence for membrane thinning effect as the mechanism for peptide-induced pore formation, Biophys. J. 84 (2003) 3751–3758.
[42] J.R. Lewis, D.S. Cafiso, Correlation between the free energy of a channel-forming voltage gated peptide and the spontaneous curvature of bilayer lipids, Biochemistry 38 (1999) 5932–5938.
[43] S. Bransburg-Zabary, A. Kessel, M. Gutman, N. Ben-Tal, Stability of an ion channel in lipid bilayers: implicit solvent model calculations with gramicidin, Biochemistry 41 (2002) 6946–6954.
[44] I. Vodyanoy, J.E. Hall, T.M. Balasubramaniam, Alamethicin-induced current–voltage curve asymmetry in lipid bilayers, Biophys. J. 42 (1983) 71–82.
[45] G. Molle, J.-Y. Dugast, G. Spach, H. Duclohier, Ion channel stabilization of synthetic alamethicin analogs by rings of inter-helix h-bonds, Biophys. J. 70 (1996) 1669–1675.
[46] A. Kessel, D.P. Tieleman, N. Ben-Tal, Implicit solvent model estimates the stability of model structures of the alamethicin channel, Eur. Biophys. J. 33 (2004) 16–28.
[47] H.W. Huang, Deformation free energy of bilayer membrane and its effect on gramicidin channel lifetime, Biophys. J. 50 (1986) 1061–1071.